

This document was prepared in conjunction with work accomplished under Contract No. DE-AC09-96SR18500 with the U. S. Department of Energy.

DISCLAIMER

This report was prepared as an account of work sponsored by an agency of the United States Government. Neither the United States Government nor any agency thereof, nor any of their employees, nor any of their contractors, subcontractors or their employees, makes any warranty, express or implied, or assumes any legal liability or responsibility for the accuracy, completeness, or any third party's use or the results of such use of any information, apparatus, product, or process disclosed, or represents that its use would not infringe privately owned rights. Reference herein to any specific commercial product, process, or service by trade name, trademark, manufacturer, or otherwise, does not necessarily constitute or imply its endorsement, recommendation, or favoring by the United States Government or any agency thereof or its contractors or subcontractors. The views and opinions of authors expressed herein do not necessarily state or reflect those of the United States Government or any agency thereof.

Paper 06637

“VAPOR SPACE AND LIQUID/AIR INTERFACE CORROSION OF LOW CARBON STEEL IN COMPLEX HIGH
LEVEL RADIOACTIVE WASTE SOLUTION”

(Karthik H. Subramanian and Bruce J. Wiersma)

STG 41

Corrosion in Nuclear Systems (TEG 224X)

VAPOR SPACE AND LIQUID/AIR INTERFACE CORROSION OF LOW CARBON STEEL IN COMPLEX RADIOACTIVE HIGH LEVEL RADIOACTIVE WASTE

Karthik H. Subramanian and Bruce J. Wiersma
Westinghouse Savannah River Company
Savannah River Site
Aiken SC 29808

ABSTRACT

Radioactive waste is stored in underground storage tanks at the Department of Energy (DOE) Savannah River Site (SRS). Recent experience has shown that steel not in contact with the bulk waste solution or slurry, but exposed to the “vapor space” above the bulk waste, may be vulnerable to the initiation and propagation of corrosion, including pitting and stress corrosion cracking, in spite chemistry controls. Experiments have now been completed in complex radioactive waste simulants, in addition to the prior experiments in simple nitrate, nitrite, hydroxide solutions. The solution chemistries tested included minor waste constituents in addition to the NaNO_3 , NaNO_2 , and NaOH which comprise the bulk of the high level radioactive waste. The additional constituents were the sodium salts of aluminate, carbonate, sulfate, phosphate, chloride, chromate, and fluoride; and nitrate salts of transition metals, typically found in the high level waste. The results indicate (1) Minor (i.e. non-reportable) and isolated pitting is possible within crevices vapor space of the tanks that contain low levels of stagnant dilute solution for an extended period of time and (2) Liquid/air interfacial corrosion is possible in dilute stagnant solutions, particularly with high chloride concentrations. However, it is clear that when stagnant conditions with high concentrations of aggressive species exist at the boundary conditions of the chemistry control program, localized corrosion, particularly at the liquid/air interface may pose a vulnerability.

Keywords: pitting, carbon steel, high level waste tank

INTRODUCTION AND BACKGROUND

Radioactive waste is stored in underground storage tanks at the Department of Energy (DOE) Savannah River Site (SRS). The waste tanks, made of ASTM A537 steel, store a combination of salts, consisting primarily of sodium nitrate, sodium nitrite, and sodium hydroxide. An assessment of the potential degradation mechanisms of the high level waste (HLW) tanks determined that nitrate-induced pitting corrosion and stress corrosion cracking were the two most significant degradation mechanisms. Specifically, nitrate-induced stress corrosion cracking was determined to be the principal degradation mechanism for the primary tank steel. Sodium hydroxide and nitrite are used to inhibit nitrate-induced stress corrosion cracking and nitrate-induced pitting corrosion in the liquid phase of the waste tanks. General corrosion is also prevented by the inhibitor levels specified for these two localized corrosion modes. The corrosion control program is based upon empirical data used to determine vulnerability to stress corrosion cracking and pitting at typical compositions of waste.¹

Recent experience has shown that steel not in contact with the bulk waste solution or slurry, but exposed to the “vapor space” above the bulk waste, may be vulnerable to the initiation and propagation of corrosion, including pitting and stress corrosion cracking. Degradation is also possible at the liquid-vapor interface due to hydroxide depletion, particularly when the interface has remained stagnant for long periods of time.

Proposed Vapor Space Corrosion (VSC) Mechanism

It was hypothesized that general or localized corrosion may occur in the vapor space due to conditions created by relative humidity and the deliquescence behavior of aggressive species. Several mechanisms have been proposed for the deposition of aggressive species on the tank wall within the vapor space. In dry environments the salt may exist as a solid residue on the

steel tank, left by evaporation or decanting of supernate. Alternatively, species may have been deposited on the tank wall by evaporation from the supernate, transport as an aerosol, and then condensation on the tank wall. In sufficiently humid conditions the residue can adsorb atmospheric moisture and dissolve, forming a corrosive electrolyte. A schematic of these mechanisms is shown in Figure 1.

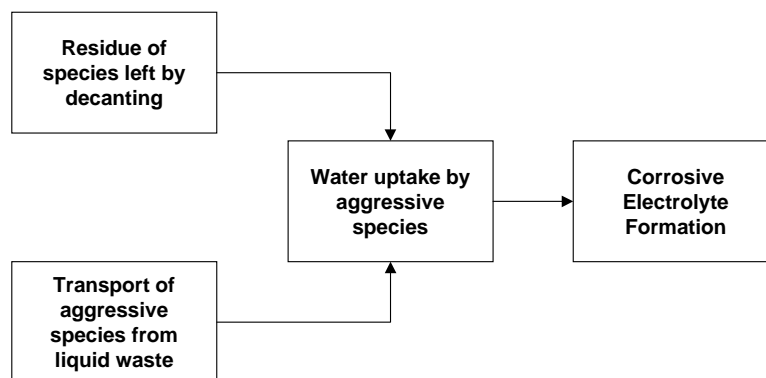


FIGURE 1: Hypothesized VSC Mechanism

It may be assumed the relative humidity of the vapor space is maintained at atmospheric humidity due to the purge ventilation systems. The HLW tanks are equipped with a purge ventilation system to maintain the tank contents at negative pressure to prevent the release of radioactive material into the environment and also to prevent the buildup of flammable vapor above the critical levels. Diurnal variation in the relative humidity, similar to daily atmospheric humidity fluctuations, may alternately dissolve and crystallize sodium nitrate, especially in the summer, when morning air is near saturation (100% RH) and afternoon heating lowers the RH below 60%. This cyclic exposure may render the steel more vulnerable than it might be under static conditions, as the cyclic exposure may tend to concentrate aggressive species depending on the precipitation sequence.

Liquid-Vapor Interface Environment and Degradation

At the vapor-liquid interface, caustic solution pH will drop naturally over a period of a few months to pH 10 due to chemical reaction of the hydroxide with atmospheric carbon dioxide. The shift in pH makes this interface region vulnerable to pitting corrosion and possibly crevice corrosion. Mechanistically, aggressive anion concentration cells may develop at stagnant vapor/liquid interfaces to accelerate corrosive attack. This type of attack is also known as waterline or beach-line attack. Oxygen concentration cells may develop as oxygen is readily available at the vapor/liquid interface, but has increasingly restricted access to levels more distant from the surface. The concentration gradient anodically polarizes the area of the tank wall slightly below the surface. This polarization leads to preferential dissolution of tank wall material at this area. Dissolved metal can then react with hydroxide, which is cathodically produced at the liquid/vapor interface, to form corrosion products that precipitate just below the water line. These deposits further retard the diffusion of oxygen and accelerate the dissolution of the tank metal. In tanks with constant waste levels, pitting corrosion could be a severe source of degradation. Previous research has shown that the inhibitor depletion at the liquid-vapor interface could lead to attack. The experimentation detailed herein would be used to validate and augment those results.

Experimental Data to Date

The initial experiments were performed in simple nitrate/nitrite/hydroxide solutions to determine the potential for vapor space and liquid/air interface corrosion of ASTM A285-70 and ASTM A537-C1.1 steels.² The material surface characteristics, i.e. mill-scale, polished, were found to play a key role in the pitting response. The results showed that the potential for limited vapor space and liquid/air interface pitting exists at 1.5M nitrate solution when using chemistry controls designed to prevent stress corrosion cracking. The key observation was that the mill scale surface with inhomogeneities could provide crevices in which the local solution chemistry could vary even if the bulk solution was controlled to prevent nitrate induced pitting, particularly in the vapor space or at the liquid/air interface.

Further experiments in simple solutions quantified pitting rates as a function of material surface characteristics, including mill-scale and defects within the mill-scale. The pitting rates were a maximum of 3 mpy for exposure above inhibited solutions, as calculated from the limited exposure times. This translated to a penetration time of 166 years for a 0.5-in tank

wall provided that the pit growth rate remains constant and the bulk solution chemistry remains constant and stagnant. The results suggest that inhibited bulk solution chemistry does not ensure pitting protection within the vapor space when there are surface inhomogeneities. However, the characteristic residual salts on the steel play a key role in the pitting characteristics.³

Experiments have now been completed in complex radioactive waste simulants. The solution chemistries tested included minor waste constituents in addition to the NaNO_3 , NaNO_2 , and NaOH which comprise the bulk of the high level radioactive waste. The additional constituents were the sodium salts of aluminate, carbonate, sulfate, phosphate, chloride, chromate, and fluoride; and nitrate salts of transition metals, typically found in the high level waste.

EXPERIMENTAL PROCEDURE

Coupon exposure testing was performed on ASTM A537-C1.1 (normalized) steel in the vapor space and the liquid/air interface within the framework of a parametric test matrix including surface conditions and solution chemistry as variables.

The testing in the vapor space was done on metallurgically mounted ¼-in. thick round disk coupons. The liquid air interfacial testing was done on 2-in x 1-in x 0.125 in. standard pitting coupons. A photograph of the experimental test setup is shown in Figure 2. The insets give higher magnification of the coupons exposed to the vapor space and the coupons exposed to the liquid/air interface.

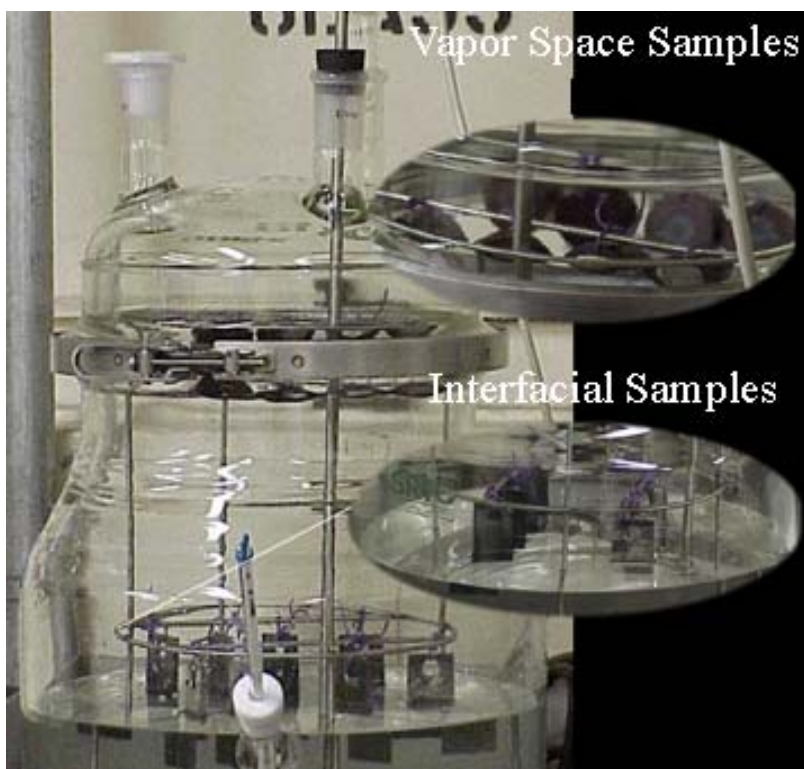


FIGURE 2: Experimental Test Setup

The bulk solution temperature was maintained at 50°C.

Steel Specifications

The tanks were fabricated with semi-killed, hot-rolled A537-C1.1 plate, with nominal composition shown in TABLE 1. The A537 steel is a ferritic/pearlitic steel with the microstructure shown in FIGURE 3. A representative coupon is shown in FIGURE 4.

TABLE 1: Steel Specifications

Steel Specification	C _{max} (wt%)	Mn (wt%)	P _{max} (wt%)	S _{max} (wt%)
ASTM A537	0.24	0.7-1.35	0.035	0.035

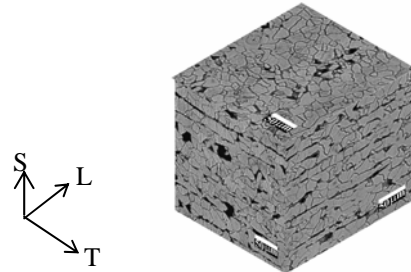


FIGURE 3: Microstructure of ASTM A537 Cl.1 Steel.

The tanks were made from hot-rolled plate and tend to have manganese sulfide and aluminum oxide inclusions that are oriented parallel to the rolling direction. Previous experiments have shown that pitting on polished coupons above simple waste simulatant has initiated in rows suspected to be in line with these inclusions.³ Other studies revealed that nitrate-induced pitting in these steels typically initiates around manganese sulfide or aluminum oxide inclusions.⁴

Surface Characteristics

The surface characteristics of the coupons of the steel were varied in terms of surface oxidation and solution deposits. The surface was oxidized by heat treatment at 975°C to simulate mill-scale, and defects in the mill scale were induced utilizing a diamond tip glass drill bit. A representative array of indents is shown in FIGURE 5. The indents exposed the underlying bare metal, and crushed the oxidized layer into the indent. The surface area of the exposed bare metal was not quantified. Deposits of the bulk solution were made on the coupon surface to simulate the mechanism of salt deposition through decanting. Testing was performed within the framework of a parametric test matrix consisting of these key variables as summarized in Table 2.

TABLE 2: Summary of Variables Tested

<u>Surface</u>	<u>Defects</u>	<u>Chemistry</u>
Mill scale	No indents	No deposit
Polished	Indents	Deposits



FIGURE 4: Representative Pitting Coupon

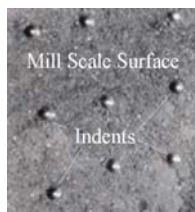


FIGURE 5: Representative Array of Microindents

Exposure Solution Chemistry

The solution chemistries tested included minor waste constituents in addition to the NaNO_3 , NaNO_2 , and NaOH which comprise the bulk of the high level radioactive waste. The additional constituents were the sodium salts of aluminate, carbonate, sulfate, phosphate, chloride, chromate, and fluoride; and nitrate salts of transition metals, typically found in the high level waste. The effect of these constituents on the corrosion response in aqueous conditions, i.e. general corrosion, pitting, stress corrosion cracking or inhibition, of low carbon steel is shown in Table 3.⁵

TABLE 3: Ion Effects on Corrosion of Low Carbon Steel

Ion	Concentration Range, M	Possible Effect
NO_3^-	1.6 - 4.5	Cracking, Pitting, General Corrosion
NO_2^-	0 - 3	Inhibition (pitting in very dilute solutions)
OH^-	0 - 5	Inhibition, Cracking at high temperature
$\text{Al}(\text{OH})_4^-$	0.4 - 1.6	Inhibition with the presence of OH^-
$(\text{CO}_3)^{2-}$	<0.1 - 0.3	Inhibition
SO_4^{2-}	0.02 - 0.2	Pitting
PO_4^{3-}	0.01 - 0.08	Inhibition
Cl^-	0.005 - 0.11	Pitting
CrO_4^{2-}	0.001 - 0.009	Inhibition
F^-	0.001 - 0.004	Pitting

In addition to the unique effects of the anions, there are significant synergistic and temperature effects on the corrosivity of the anions. For, example, nitrate is known to cause stress corrosion cracking of steel at intermediate and high temperatures, and significant general corrosion at low temperatures. Hydroxide can cause stress corrosion cracking of steels at high temperatures, provided that the concentration is high enough. However, with control of the solution temperature and nitrate to hydroxide ratios, stress corrosion cracking can be prevented. This is complex condition created due to the stability of the surface film on the steel as a function of the cathodic reaction. In the case of nitrate reduction on the surface, cracking is promoted, whereas oxygen reduction reduces the propensity for cracking, but increases general corrosion. However, the addition of hydroxide promotes a stable film that prevents nitrate general corrosion. In high hydroxide conditions, the addition of nitrate at some intermediary level where oxygen reduction is the preferred reaction prevents the electrochemical conditions that can promote caustic stress corrosion cracking.⁶

Four solutions were chosen for testing. Solutions 1 and 2 had the minimum inhibitor requirements as bound by the current chemistry control program, $\text{NaNO}_3 = 1.5\text{M}$, $\text{NaNO}_2 = 0.45\text{M}$, and $\text{NaOH} = 0.15\text{M}$. In addition, solution 1 had all the aggressive anions at the maximum concentrations, and solution 2 contained aggressive anions at the maximum concentrations and inhibiting ions at the minimum concentrations. Solutions 3 and 4 were chosen from the latest samples received from

actual tanks. These tanks were chosen for several reasons. These tanks have been known to have the highest temperatures (Tank 'T') as well as purge ventilation failures (Tank 'P') that indicate vapor space activity.⁷ A summary of the salt concentrations of the solution chemistries tested is shown in TABLE 4.

TABLE 4: Concentrations in Moles of Solution Chemistries Tested

Compound	Formula	Solution 1	Solution 2	Tank T	Tank P
Sodium Hydroxide	NaOH	0.15	0.15	6.66	2.6
Sodium Carbonate, Monohydrate	Na ₂ CO ₃ •H ₂ O	0.100	0.100	0.120	0.270
Sodium Nitrite	NaNO ₂	0.450	0.450	1.175	0.641
Sodium Nitrate	NaNO ₃	1.5	1.5	2.6246	1.8
Aluminum Nitrate	Al(NO ₃) ₃ •9H ₂ O	0.005	0.005	0.41	0.21
Sodium Chloride	NaCl	0.11	0.11	0.023	0.0066
Sodium Sulfate, Decahydrate	Na ₂ SO ₄ •10H ₂ O	0.2	0.2	0.027	0.0464
Sodium Fluoride	NaF	0.01	0.01	0.005	0.0059
Sodium Oxalate	Na ₂ C ₂ O ₄	0.002	0.002	0.0057	0.0064
Sodium Chromate, Anhydrous	Na ₂ CrO ₄		0.001		
Sodium Molybdate, Dihydrate	Na ₂ MoO ₄ •2H ₂ O		0.002		
Sodium meta-Silicate, 9 Hydrate	Na ₂ SiO ₃ •9H ₂ O				
Sodium Phosphate, Tribasic	Na ₃ PO ₄ •12H ₂ O		0.01	0.0097	0.0059

A summary of the transition metal concentrations are shown in TABLE 5.

TABLE 5: Transition Metal Concentration in Solution Chemistries Tested

Compound	Chemical Formula	Concentration [M]
Ferric Nitrate	Fe(NO ₃) ₃ •9H ₂ O	0.0248
Cupric Sulfate	CuSO ₄ •5H ₂ O	0.0043
Mercuric Nitrate	Hg(NO ₃) ₂ •H ₂ O	0.025
Nickel Nitrate	Ni(NO ₃) ₂ •6H ₂ O	0.0015
Cobalt Nitrate	Co(NO ₃) ₂ •6H ₂ O	0.003
Chromium Chloride	CrCl ₃ •6H ₂ O	0.00375

A graphical representation of the chemistry control program is shown in FIGURE 6. The summary indicates the hydroxide and nitrite levels that are to be maintained as a function of nitrate concentration. The inhibited chemistry tested is indicated

on the graph. Limit L3, the regime within which the pitting studies were done, addresses the nitrate range that is typical of fresh waste. The limit is specified to prevent nitrate-induced stress corrosion cracking, as pitting is not expected, based primarily on engineering judgment. The limit was based upon a combination of operational experience and the knowledge of the corrosion mechanisms. A minimum hydroxide concentration of 0.1 M was conservatively selected to maintain inhibiting conditions in 1M nitrate waste solutions. The minimum hydroxide concentration and the minimum sum of hydroxide and nitrite in L3 over the range 1 M nitrate to 2.75 M nitrate were selected to transition smoothly to the L2 limit at 2.75 M nitrate. Limit L3 carries a maximum temperature of 70°C, or 105°C if the sum of hydroxide and nitrite concentrations exceeds twice the nitrate concentration.

The pitting studies were conducted within this regime as it is expected to be the most aggressive contributing to pitting in the vapor space and at the interface, particularly at the boundary conditions tested. The limited hydroxide and nitrite availability at the interface may lead to pitting at the interface due to inhibitor depletion during extended periods of waste level stagnancy. Additionally, the limited hydroxide availability may diminish the hypothesized inhibitive effect of hydroxide within the vapor space. The testing was conducted at the boundary conditions to provide a conservative approximation of pitting rates, even though the tanks are currently operated at much high hydroxide concentrations.

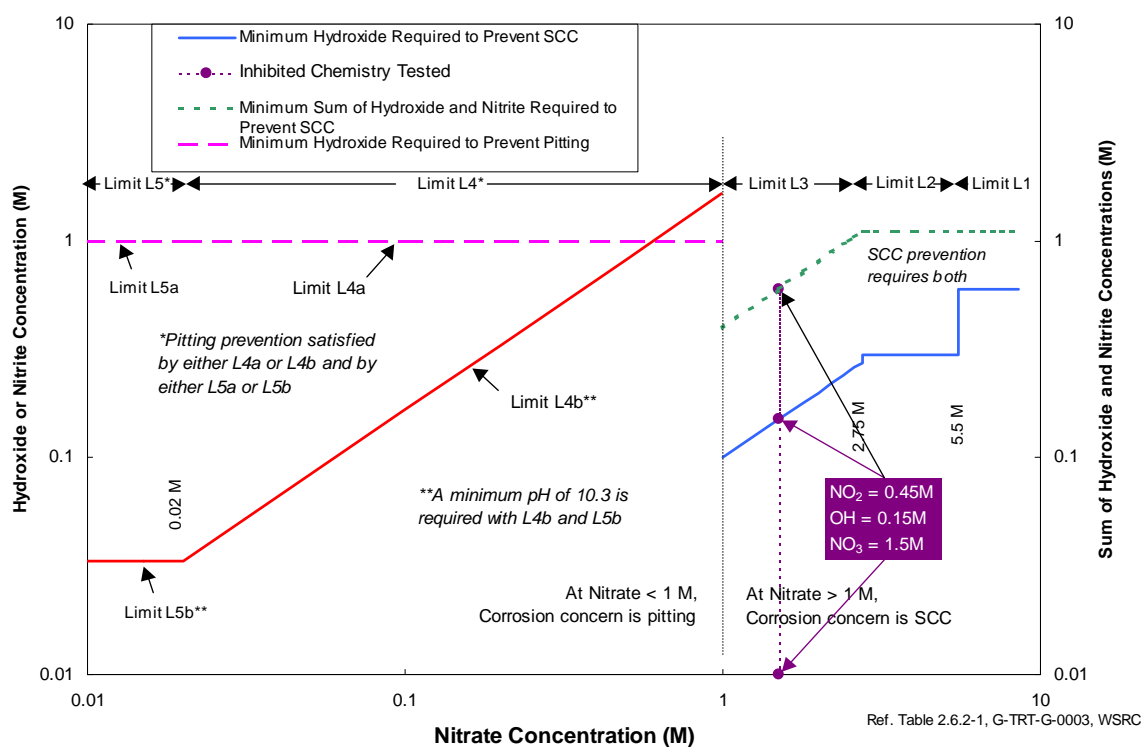


FIGURE 6: Summary of Chemistry Control Program and Chemistry Tested

The possibility of pitting of carbon steel by the nitrate ion has been the most studied in laboratory testing of dilute (hydroxide and nitrate concentrations < 1 molar) simulated radioactive waste solutions. This minimum nitrite concentration was found to vary linearly with the concentration of the test solution and to depend empirically on the Celsius temperature exponentially.⁸ When nitrate, chloride, or sulfate was varied independently of the other waste simulant components, the familiar linear relationship was found between the logarithm of the inhibiting nitrite concentration and the logarithm of the aggressive species concentration.⁹ Nitrate controls the minimum nitrite requirement to prevent pitting in certain high-level radioactive waste solutions because it is the most abundant aggressive ion in those solutions.

RESULTS

The coupons were analyzed for pit location and pit depth, when possible. An average pit depth and a corresponding pitting rate were determined when appropriate. The following section presents the results of the testing for solution 1,

solution 2, Tank T solution, and Tank P solution. Each of the section presents the solution racks as they were removed from exposure, the vapor space coupons, and the liquid-air interface coupons.

Solution 1 Results

The solution rack as removed from exposure is shown in FIGURE 7.



FIGURE 7: Solution 1 Solution Rack as Removed.

The visual analysis of the vapor space coupons, shown in Figure 8 revealed severe corrosion on the polished specimens with the initial deposits, but only spotty corrosion on polished specimens without the initial deposits. The heat treated coupons exhibited severe corrosion only when deposits and indents were both present. The other coupons exhibited spotty corrosion, but were largely protected. It is important to note that the indented coupon without the deposit did not exhibit corrosion.

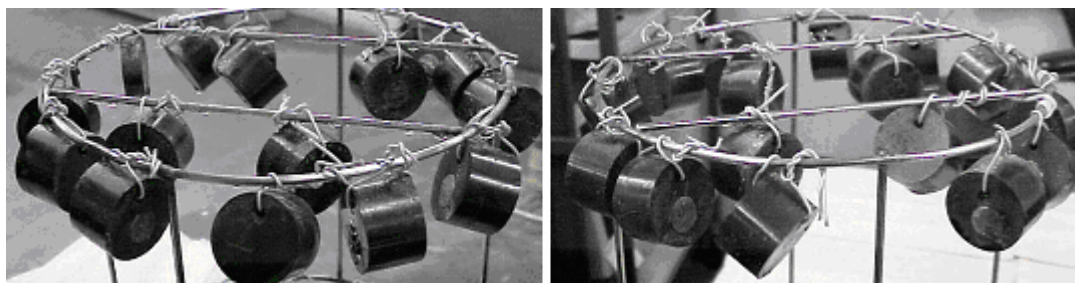


FIGURE 8: Vapor Space Coupons as Removed from Exposure to Solution 1.

The polished specimens of the liquid air coupons were severely corroded above the line and moderately corroded below the line. The below the line corrosion was limited to the “outer surface” of the coupon, while the “inner surface” of the coupons appeared uncorroded. This may be due to liquid level stagnancy on the outer surface, since the stirring motion within the cell was limited to the center of the cell. The coupons are then presented after cleaning in Clarke’s solution, once again with the inner surface first, and the outer surface following. The polished coupons had a significant amount of corrosion just above the liquid level including growth of the oxide scale approximately $\frac{1}{4}$ ” from the surface of the coupon. However, corrosion below the level was limited to the outer surface of the coupon where liquid was stagnant. The heat treated coupons exhibited a similar growth of oxide scale and delamination of the heat treatment layer.

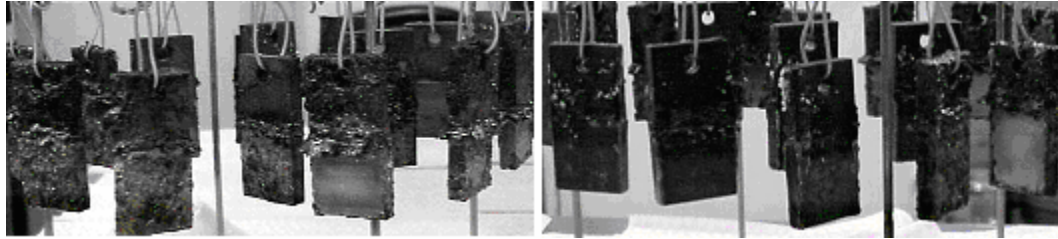


FIGURE 9: Liquid/Air Interface Coupons as Removed from Exposure to Solution 1.

Solution 2 Results

The solution rack as removed from exposure is shown in FIGURE 7.

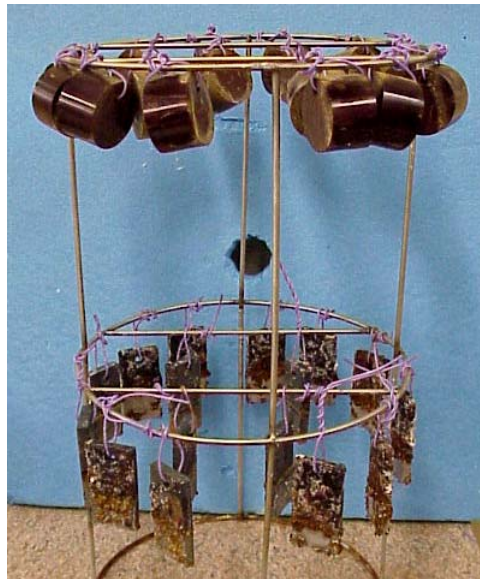


FIGURE 10: Solution 2 Rack as Removed.

The visual analysis of the vapor space coupons revealed severe corrosion on the polished specimens with the initial deposits, but only spotty corrosion on polished specimens without the initial deposits. The heat treated coupons exhibited severe corrosion only when deposits and indents were both present. The other coupons exhibited spotty corrosion, but were largely protected. It is important to note that the indented coupon without the deposit did not exhibit corrosion.

The polished specimens of the liquid air coupons were severely corroded above the line and moderately corroded below the line. The below the line corrosion was limited to the “outer surface” of the coupon, while the “inner surface” of the coupons appeared uncorroded. This may be due to liquid level stagnancy on the outer surface, since the stirring motion within the cell was limited to the center of the cell. The polished coupons had a significant amount of corrosion just above the liquid level including growth of the oxide scale approximately $\frac{1}{4}$ ” from the surface of the coupon. However, corrosion below the level was limited to the outer surface of the coupon where liquid was stagnant. The heat treated coupons exhibited a similar growth of oxide scale and delamination of the heat treatment layer.

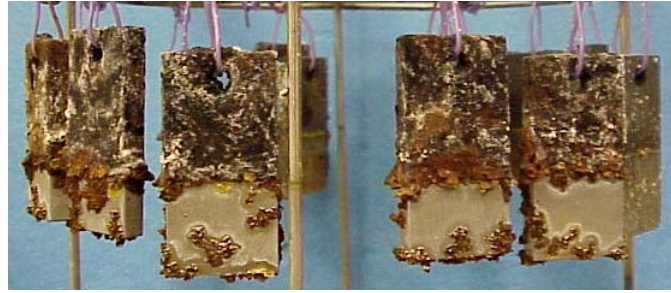


FIGURE 11: Solution 2 Liquid/Air Interface Coupons as Removed.

Tank T Results

The coupons as removed from the test solutions are shown on the coupon rack in FIGURE 12.



FIGURE 12: Tank T Rack as Removed

The vapor space coupons and liquid/air interfacial coupons are shown in FIGURE 13 and FIGURE 14 respectively. The coupons exhibit only minor staining and there is no evidence of localized or general corrosion.



FIGURE 13: Vapor Space Coupons from Tank T Solution Exposure



FIGURE 14: Liquid/Air Interface Coupons from Tank T Solution Exposure

Tank P Results

The coupon rack as removed from the Tank P solution is shown in FIGURE 15



FIGURE 15: Coupon Rack as Removed from Tank P Solution

The vapor space and liquid/air interfacial coupons as removed from the solution are shown in FIGURE 16 and FIGURE 17 respectively. Once again, it is seen that there is minor staining and no corrosion on any of the coupons. In fact, many of the coupons retained their initial shiny condition.



FIGURE 16: Vapor Space Coupons as Removed from Tank P Solution Exposure.



FIGURE 17: Liquid/Air Interface Coupons as Removed from Tank P Solution Exposure.

DISCUSSION

The key goal of this testing was to determine the effect of the minor waste constituents on the corrosion response of the tank steel. It is clear from the testing that the minor waste constituents greatly influence the pitting and corrosion response of the steels, specifically at the boundary conditions of the chemistry control program and when the concentration of the proposed aggressive species, for example chlorides are high. The vapor space and liquid/air interface coupons exposed to solutions 1 and 2, in which the chlorides are at high concentrations and inhibitors were low, exhibited extensive general corrosion and pitting.

The pitting in the vapor space coupons exposed to solutions 1 and 2 could not be quantified, but some general observations were made. The polished vapor space coupons exposed to solution 1 and solution 2 are shown in FIGURE 18 and FIGURE 19 respectively. These figures show the coupons with no surface modifications, the coupon with a surface deposit, the coupon with indents, and the coupons with the deposit and the indent ('D + I'). It is seen that the coupons with the deposits exhibited extensive corrosion, but there didn't appear to be any significant transport of the salts to the vapor space during the test period. These results were similar to those of solution 2. The results suggest that decanting of the solution and the consequent residual species may be the primary parameter mechanism by which aggressive species may be available for corrosion in the vapor space. In addition, the extent to which the initial solution is inhibited prior to decanting of the solution plays a key role in the corrosion in the vapor space. In this case, the final solution pH was measured to be 9.8 and 9.9 for solution 1 and solution 2 respectively, but still did not lead to transport of the species into the vapor space. The indented coupons were broadly corroded and the indents did not provide any specific location for extensive corrosion as expected for the polished specimens.



FIGURE 18: Polished Vapor Space Coupons Exposed to Solution 1.



FIGURE 19: Polished Vapor Space Coupons Exposed to Solution 2

The heat treated coupons for vapor space coupons exposed to solutions 1 and 2 exhibited minor corrosion only in the indented specimens and specifically when surface deposits were present. These results are shown in FIGURE 20 and FIGURE 21 for solution 1 and solution 2 respectively.

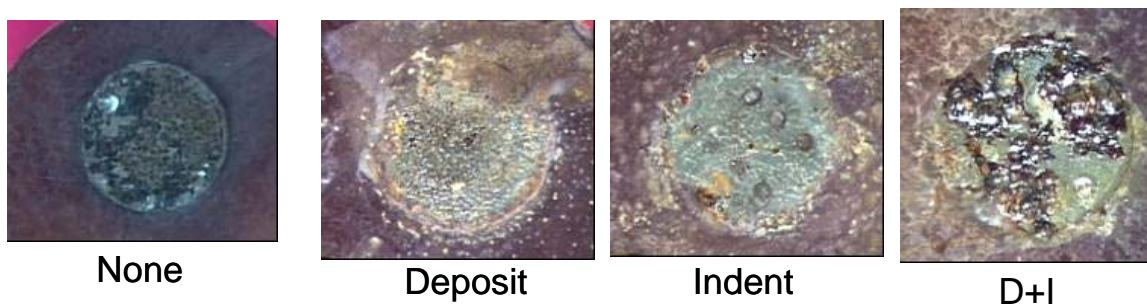


FIGURE 20: Heat Treated Vapor Space Coupons Exposed to Solution 1.



FIGURE 21: Heat Treated Vapor Space Coupons Exposed to Solution 2.

The pitting in the liquid/air interface coupons exposed to solutions 1 and 2 were measured and corresponding corrosion rates were determined. The pitting rates were calculated below the liquid line, at the liquid line, and just above the liquid line. The results for the polished coupons are shown in FIGURE 22 and FIGURE 23 for solutions 1 and 2 respectively. The results indicate that the pitting rates are between 6-10 mpy for solution 1 while 3-6 for solution 2. In addition, the pitting rates were higher and sometimes only measurable above the line for solution 2 while evident for solution 1. These results suggest that even minimum quantities of minor waste constituents known to be corrosion inhibitors, such as chromate and phosphate, reduce the corrosion rate. This is further corroborated by the fact that the heat treated coupons exposed to solution 2 remained protected, while those exposed to solution 1 exhibited pitting as shown in FIGURE 24.

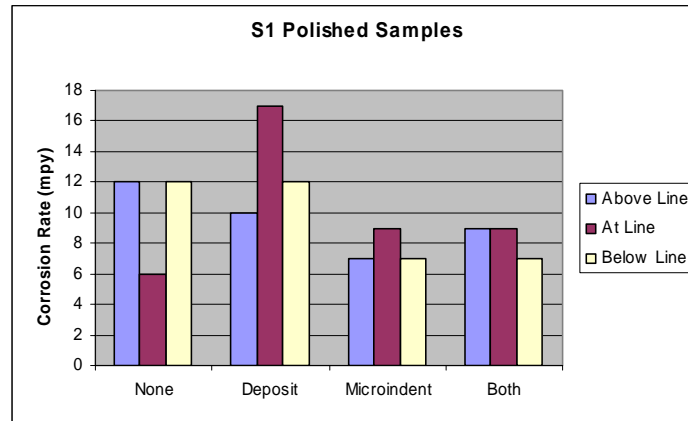


FIGURE 22: Pitting Rates for Liquid/Air Interface Coupons Polished Exposed to Solution 1.

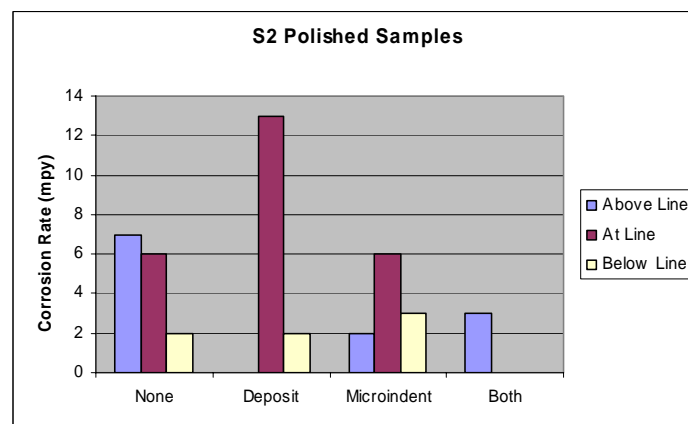


FIGURE 23: Pitting Rates for Liquid/Air Interface Polished Coupons Exposed to Solution 2.

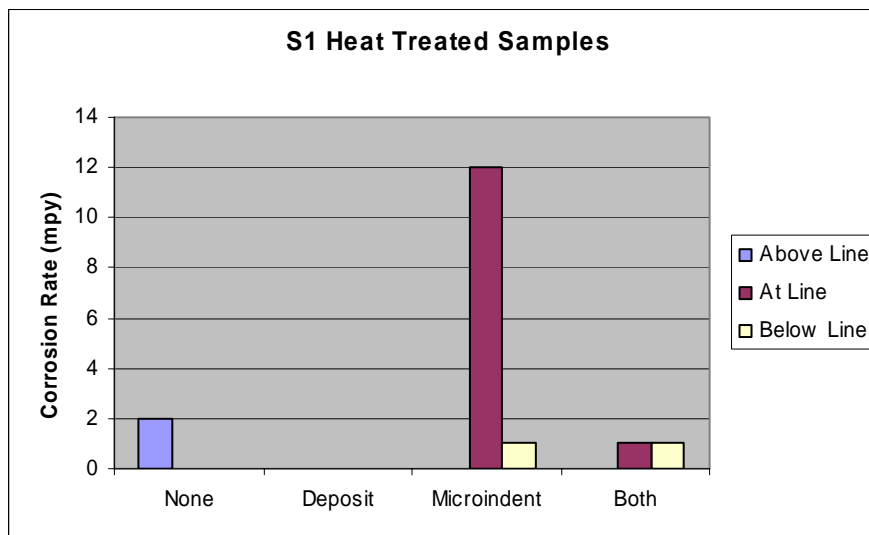


FIGURE 24: Pitting Rates for Liquid/Air Interface Heat Treated Coupons Exposed to Solution 1.

The coupons exposed to solutions typical of Tank T and Tank P revealed no measurable corrosion on the polished specimens. In addition, the heat treated coupons were well protected, and also revealed no measurable corrosion.

SUMMARY AND CONCLUSIONS

Radioactive waste is stored in underground storage tanks at the Department of Energy (DOE) Savannah River Site (SRS). Recent experience has shown that steel not in contact with the bulk waste solution or slurry, but exposed to the "vapor space" above the bulk waste, may be vulnerable to the initiation and propagation of corrosion, including pitting and stress corrosion cracking, in spite chemistry controls.

Experiments have now been completed in complex radioactive waste simulants, in addition to the prior experiments in simple nitrate, nitrite, hydroxide solutions. The solution chemistries tested included minor waste constituents in addition to the NaNO_3 , NaNO_2 , and NaOH which comprise the bulk of the high level radioactive waste. The additional constituents were the sodium salts of aluminate, carbonate, sulfate, phosphate, chloride, chromate, and fluoride; and nitrate salts of transition metals, typically found in the high level waste.

The results indicate the following in solutions typical of waste tanks:

- Minor (i.e. non-reportable) and isolated pitting is possible within crevices vapor space of the tanks that contain low levels of stagnant dilute solution for an extended period of time
- Liquid/air interfacial corrosion is possible in dilute stagnant solutions, particularly with high chloride concentrations

However, it is clear that when stagnant conditions with high concentrations of aggressive species exist at the boundary conditions of the chemistry control program, localized corrosion, particularly at the liquid/air interface poses a vulnerability.

ACKNOWLEDGMENTS

The author would like to thank Karen Hicks for technician support and performing the experiments. Additionally, the author thanks J.I. Mickalonis, P.E. Zapp, and A.J. Duncan for technical assistance.

REFERENCES

- [¹] K.H. Subramanian and P.E. Zapp, "Review of Inhibition of High Level Radioactive Waste Tanks in the DOE Complex," CORROSION/2004, Paper No. 04420, NACE International, Houston TX 2004.
- [²] K. H. Subramanian and P. E. Zapp, "Investigation of the Corrosivity of the Vapor Phase Over High Level Radioactive Waste," CORROSION/2003, Paper No. 03676, NACE International, Houston TX, 2003.
- [³] K.H. Subramanian and P.E. Zapp, "Pitting Corrosion in the Vapor Space and Liquid/Air Interface of High Level Radioactive Waste Tank," CORROSION/2004, Paper No. 04683, NACE International, Houston TX, 2004.
- [⁴] J.I. Mickalonis, "Corrosion of Steel in Simulated Nuclear Waste Solutions," Paper No. 117, NACE International, Houston, 1994.
- [⁵] R.S. Ondrejcin, "Prediction of Stress Corrosion of Carbon Steel by Nuclear Process Liquid Wastes," DP-1478, E.I. Dupont Nemours and Co., August 1978.
- [⁶] K.H. Subramanian and J.I. Mickalonis., "Anodic Polarization Behavior of Low Carbon Steel in Concentrated Sodium Hydroxide Solutions with Sodium Nitrate Additions," Electrochemica ACTA, December 2004.
- [⁷] K.H. Subramanian and C.F. Jenkins, "Failure Analysis of Tank 39 Purge Ventilation System Vent Pipe," Practical Failure Analysis, May 2004.
- [⁸] P.E. Zapp and D.T. Hobbs, "Inhibiting Pitting Corrosion in Carbon Steel Exposed to Dilute Radioactive Waste Slurries, CORROSION/92, paper no. 98, Houston TX, NACE International 1992.

[⁹] J.W. Congdon, "Inhibition of Nuclear Waste Solutions Containing Multiple Aggressive Anions," *Materials Performance*, 15, p.34, 188.